

# Density Functional Theory Studies of Graphene

A Dissertation for  
PHY-651 Dissertation

Credits: 16

Submitted in partial fulfillment of Masters Degree  
M.Sc in Physics (Computational Physics)

Goa University  
in the subject of Physics  
by

NASHLEY .A. DIAS  
Seat number: 22P0430022  
ABC id : 952-948-129-121

Under the supervision of  
PRN: 20192570

**BHARGAV.K.ALAVANI**

School Of Physical and Applied Science  
Physics discipline



Goa University

April 2024



Examined by:

Seal of the School

## DECLARATION

I hereby declare that the data presented in this Dissertation report entitled, “ Density Functional Theory Studies of Graphene ” is based on the results of investigations carried out by me in the Master of Science in Physics Discipline at the School of Physical and Applied Science, Goa University under the Supervision of Dr. Bhargav.K.Alavani and the same has not been submitted elsewhere for the award of a degree or diploma by me. Further, I understand that Goa University or its authorities will not be responsible for the correctness of observations / experimental or other findings given the dissertation.

Date: 9 May 2024

Place: Goa University

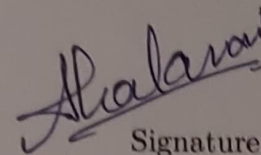
Name: Nashley.A.Dias

Seat Number: 22PO430022

Signature: 

## Completion certificate

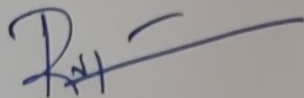
This is to certify that the dissertation report “ Density Functional Theory Studies of Graphene” is a bonafide work carried out by Mr Nashley Angelo Dias under my supervision in partial fulfilment of the requirements for the award of the degree of Masters in Science in the Discipline of Physics at the School of Physical and Applied Science, Goa University.



Signature:

Name of Supervisor: Bhargav.K.Alavani

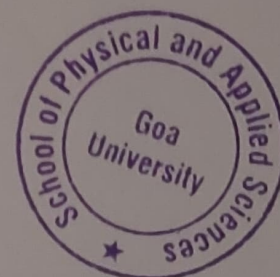
Date: 9 May 2024



Signature of HoD for Physics :

Date 9/5/24.

Place: Goa University



School stamp

## ACKNOWLEDGEMENT

I would like to express my gratitude to my project guide Dr. Bhargav Alavani for his guidance and constant support to the completion of my project titled Density Functional Theory Studies of Graphene. I would like to acknowledge the support of my colleagues and the faculty for providing the resources and support for the completion of my project

# Contents

<b>1 Introduction</b>	<b>2</b>
1.1 Literature Review	2
1.2 Objectives	3
<b>2 Methodology</b>	<b>4</b>
2.1 Hamiltonian of n electron system	4
2.2 APPROXIMATIONS	5
2.2.1 HARTREE FOCK method	5
2.2.2 Success and failure of Hartree-Fock	6
2.3 <i>Density Functional Theory</i>	6
2.3.1 Electron density	6
2.3.2 Foundations of dft: Kohn-Hohenberg theorems	6
2.3.3 Reformulation of the Hamiltonian using Kohn Hohenberg theorems	6
2.3.4 Self-Consistent Field/Procedure for dft	7
2.3.5 Pseudo-potentials: a need and its types	8
2.3.6 exchange-correlational approximation	9
2.3.7 <i>limitations of LDA and GGA</i>	9
2.4 vdw correctionals	9
2.4.1 vdw-df2	10
2.4.2 vdw-df-c6 or c6	10
2.5 limitations of dft	10
<b>3 Results</b>	<b>11</b>
3.1 Mono-Layer Graphene (MLG)	11
3.1.1 structure for graphene	11
3.2 Optimization	12
3.3 excitation spectra	13
3.4 Bi-layer Graphene(BLG)	14
3.4.1 AA Stacking	15
3.4.2 AB stacking	16
3.4.3 Comparson between AA and AB stacking	18

<b>3.5 Doping</b> . . . . .	19
<b>3.5.1 Comparison between un-doped and doped MLG</b> . . . . .	19
<b>3.6 N-DOPED BI-LAYER GRAPHENE: N DOPED BLG</b> . . . . .	21
<b>3.7 Summary</b> . . . . .	25

# List of Tables

3.1 pseudopotential, approximation and lattice constant	11
3.2 optimized value for AA structure	15
3.3 Data for different vdw functionals for AA	15
3.4 band gap with different vdw functionals for AA stacking	16
3.5 lattice constant, energy obtained for different vdw functionals for AB	16
3.6 band gap with different vdw functionals for AB stacking	18
3.7 band gap for different vdw functionals with AA and AB stacking for bi-layer graphene	18
3.8 inter-layer distance in Å for <i>BLG</i>	18
3.9 pseudo-potential, approximation, and lattice constant	19
3.10 obtained bond length for N doped MLG	19
3.11 properties of undoped and doped MLG	20
3.12 N-doped AA BLG data	21
3.13 N-doped AB BLG data	21
3.14 inter-layer distance for N doped BLG with pbe	22
3.15 inter-layer distance for N doped BLG with DF2	22
3.16 inter-layer distance for N doped BLG with C6 for vdw interaction.	22
3.17 DOS and Fermi energy obtained for AA and AB stacking for pbe	22
3.18 Fermi energy and DOS obtained for AA and AB stacking with df2	25
3.19 Fermi energy and DOS obtained for AA and AB stacking with c6	25

# List of Figures

2.1	<i>different potential terms: figure 1 is the inter electron-nuclear term, figure 2 is the nuclear-nuclear term, figure 3 is the electron-electron term</i>	4
2.2	scf procedure for dft	8
3.1	structure for unit cell for MLG and its extended version 3x3x1	11
3.2	K-point graph using PAW pseudo-potential	12
3.3	ecut graph for PAW	12
3.4	smearing here for PAW	13
3.5	bandstructure of PAW	14
3.6	DOS of PAW	14
3.7	AA stacking structure: unit cell and 3x3x1	15
3.8	Band-structure for AA stacking with c6 vdw correctional and its zoomed version.-20 eV to 10 eV for the 1st image, right one is -5 to 5 eV range	16
3.9	The DOS of the above figures with the same energy range	16
3.10	AB stacking: unit cell and 3x3x1	17
3.11	Band structure for AB stacking with c6 vdw. energy range for the left one is -20 to 10 eV, right one is -5 to 5 eV	17
3.12	DOS of the above figure with the same energy range	17
3.13	relative error for inter-layer distance for AA and AB stacking for different vdw functionals; AA is blue while AB is orange.Experimental value for AA =3.55 Å and for AB=3.35 Å	18
3.14	structure of undoped and doped monolayer graphene	19
3.15	The different bond length diagram C-C ( N far), C-C(N near), N-C. atoms in green represent the selected atoms	20
3.16	band structure and DOS of undoped and doped MLG.the red line is the lowest conduction and highest valence band respectively	20
3.17	. we have used 3x3x1 repetition of the unit is used here	21
3.18	different interlayer distance for different types of bonds for AA.	22
3.19	different interlayer distance for different types of bonds for AB.	22
3.20	AA on the left-hand side and AB on the right-hand side	23
3.21	AA and AB stacking with df2 and c6 vdw correction	24

**Abbreviations Used**

1. DFT: density functional theory
2. BLG: Bi-layer Graphene
3. MLG: Mono-Layer Graphene
4. LDA: Local Density Approximation
5. GGA: Generalized Gradient Approximation
6. vdw: Van Der Waals functionals
7. DOS: Density of States
8. SCF: Self-Consistent Field or Self-Consistent Procedure
9. N: Nitrogen
10. C: Carbon

## **Abstract**

Density Functional Theory is a numerical method that simplifies the N-body electron Schrodinger equation by using electron density as a parameter. It is a go-to method to simulate the materials' electronic, optical and mechanical properties. This work is to study the effect of Nitrogen doping on the electronic properties of Mono Layer and Bilayer Graphene. Also, study how various hybrid functionals ( Van der Waals functionals ) affect the inter-layer distance with different stacking geometries and its effect on band structure.

# Chapter 1

## Introduction

2D materials as of recent are very popular due to their unique properties such as high flexibility, electrical conductivity and strength. Out of these materials Graphene is usually preferred due to the ease of synthesis, high strength and electrical conductivity. It's a popular precursor to create materials like fullerenes and reduced graphene oxide which has wide applications in sensors, energy storage, electronics and the lubrication industry. Density Functional Theory is a numerical method to solve the n-electron Schrodinger equation. This is widely used to study or predict the electronic properties of the chosen material. It's very popularly used in material science due to ease and consistent results with the experimental data obtained, although, in many cases it fails to predict correct properties.

### 1.1 Literature Review

*Hartree, and Fock* simplified the n body electron Hamiltonian and made it easy to solve for small systems however infeasible for stimulating large systems. *Kohn and Hohenberg* laid two fundamental theorems using electron density as a parameter and later improved by *Kohn and Sham* which paved the way for foundations of density functional theory which made it possible to solve it computationally and to calculate the electronic properties of the system, they also used the pseudo-potential and LDA approximation, *John Perdew, Kieron Burke, and Ernzerhof (PBE)* [1] invented GGA approximation 1996 making it easy to solve whose electron keeps on changing. *Stefan Grimme* in 2004 introduced the new-correctional functionals (dft-d or vdw-df) which were used to guess the nature of the vdw forces and have since been modified and improved on. Graphene is chosen because of its high electron conductivity, Young's modulus and high thermal conductivity also it can be used to create other C-based allotropes along with all of this it has a 0 band gap [2]. Studies carried out by *M. Boujnah* [3] on the AA and AB on pristine BI-LAYER GRAPHENE(BLG) and *A. Ahmed* [4] on the pristine and N-doped MONO-LAYER GRAPHENE with the help of PAW pseudo-potential without any vdw correctional functionals

## 1.2 Objectives

1. Investigate the properties of monolayer graphene through Density Functional Theory.
2. Study bilayer graphene with various stacking configurations.
3. Use hybrid functionals to include interlayer van der Waals interactions to increase the accuracy of calculations for bilayer Graphene.
4. Explore the influence of doping on both monolayer and bilayer graphene.

# Chapter 2

## Methodology

### 2.1 Hamiltonian of n electron system

**Hamiltonian** is used to describe the total energy for a system of particles, it is written as  $\hat{H} = \hat{T} + \hat{V}$ , where  $\hat{T}$ ,  $\hat{V}$  represent the kinetic and potential energy respectively. The Hamiltonian for n electron body (Schrodinger equation) is

$$\hat{H} = \frac{-\hbar^2}{2m} \sum_i \nabla_i^2 - \sum_A \frac{\hbar^2}{2M_A} \nabla_A^2 - \sum_{A,i} \frac{Z_A e^2}{4\pi\epsilon_0 r_{Ai}} + \sum_{A,B_{A>B}} \frac{Z_A Z_B e^2}{4\pi\epsilon_0 R_{AB}} + \sum_{i,j_{i>j}} \frac{e^2}{4\pi\epsilon_0 r_{ij}}$$

i,j represents the electron position while A, B represents the atomic nuclei position, the 1st two terms represent the kinetic energy of the system while the last 3 terms represent the potential energy of nuclei-electron, nuclei-nuclei, and electron-electron respectively

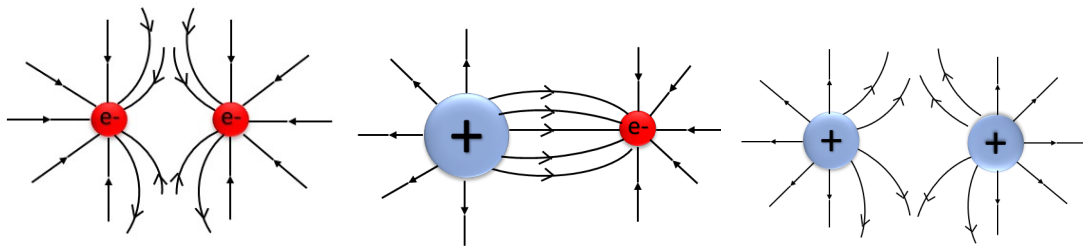


Figure 2.1: *different potential terms*: figure 1 is the inter electron-nuclear term, figure 2 is the nuclear-nuclear term, figure 3 is the electron-electron term

in the above Hamiltonian, we require a large amount of storage to store the necessary wave function, it's hard to solve the interaction term and practically impossible to know all the electron's positions in the system with high certainty

## 2.2 APPROXIMATIONS

### Born Oppenheimer Approximation

The Hamiltonian can be decoupled into the electron and nuclear Hamiltonian and their coupling term is zero

the kinetic energy of nuclear is very small with respect to the electron and the potential between two nuclei is constant and smooth in nature

### Independent Electron Approximation

the electron-electron interaction can be approximated to a mean-field

### Central Field Approximation

the mean field of this electron cloud can be approximated as a central field  $V_{cf}(\vec{r}) = V_{N,e}(\vec{R}, \vec{r}) + V_{ee}^{cf}(\vec{r})$

1st term represents the potential of electron-nuclei and 2nd term represents the electron-electron potential in a field and the Hamiltonian after all these approximations is

$$\hat{H} = \frac{-\hbar^2}{2m} \sum_i \nabla_i^2 + V_{cf}(\vec{r}) \quad [5]$$

### 2.2.1 HARTREE FOCK method

1. Hartree and Fock used a non-interacting single electron model
2. Hartree-Fock assumptions

- **born-Oppenhemier, independent electron and central field approximation are assumed**
- The electronic wave function can be written as a linear combination of single non-interacting electrons in the form of a determinant

$$\psi(\vec{q}, \vec{R}) = \frac{1}{\sqrt{N}} \begin{vmatrix} u_1(1) & \dots & u_1(n) \\ u_2(1) & u_i(q_j) & \dots \\ u_n(1) & \dots & u_n(n) \end{vmatrix} \quad (2.1)$$

- After finding the wave function, we use the variational principle subject to the condition with the wave function found as our trial wave function.

$$\delta \langle \Psi^N | H^N | \Psi^N \rangle = 0 \text{ under the constraint that } \langle u_i | u_j \rangle = \delta_{ij}$$

- we get a set of equations called Hartree fock equations, in operator form is written as

$$f(\vec{r}_1) u_i(\vec{r}_1) = \epsilon_i u_i(\vec{r}_1)$$

$$h(r_1)u_i(r_1) + \sum_j \left[ \int dV_2 \frac{u_j^*(r_2)}{r_{12}} (u_i(r_1)u_j(r_2)) - \delta(m_{s_i}, m_{s_j})(u_i(r_2)u_j(r_1)) \right] = \epsilon_i u_i(r_1)$$

$\epsilon_i$  is the energy of electron orbital,  $u_i$  is the electron orbital,  $f$  is the Hamiltonian

- the above operator behaves similar to eigenvalue equation and hence it's called a pseudo eigen equation

## 2.2.2 Success and failure of Hartree-Fock

the electronic energy, electronic wave-function, orbitals and orbital energies, account for the Pauli exclusion principle and take care of exchange-correlation terms, a good 1st order approximation for the ground-state

it underestimates the true ground-state energy with a slight modification that can be corrected to give a correct output i.e

$$E'_{HF} = \sum_i \epsilon_i + V_{ee} \quad \text{where} \quad \sum_i \epsilon_i = \sum_{i=1}^N H_i + \sum_{i,j=1}^N (J_{ij} - k_{ij})$$

Neglects electron correlation, requires high storage, not suitable for strongly correlated systems, we can't measure the wave function

## 2.3 Density Functional Theory

### 2.3.1 Electron density

We use the electron density to find the properties of the system/ and the electron density can be defined as  $n(r) = |\psi^2(r)|$  all the information is embedded in this  $\psi_{new}(r)$  which is equivalent to the old  $\psi(q, r)$ , also we use this now to solve the Schrodinger eqn

note the amount of storage is now significantly less and is better optimized to solve it

### 2.3.2 Foundations of dft: Kohn-Hohenberg theorems

**Kohn-Hohenberg 1st theorem:** it states that the external potential is uniquely determined by the ground state electron density  $n_0$ .

**Kohn Hohenberg 2nd theorem :** there exists a universal function for energy  $E_n$  in terms of electron density which it can be uniquely mapped to any external potential, the true global min of this function will give the true ground state energy and the corresponding density is the ground state density

$$E[\rho(r)] = F[\rho(r)] + E_{ext}[\rho(r)] \geq E_{gs}$$

### 2.3.3 Reformulation of the Hamiltonian using Kohn Hohenberg theorems

- using electron density as the input ,this functional(electron density ) for single particles states is

$$\text{given by } F(n(r)) = \kappa_e(n(r)) + \frac{\iint n(r)n(r')drdr'}{2|r-r'|} + \epsilon_{xc}$$

- **kohn and sham** using electron density functional. modified the Schrodinger eqn to get

$$E[n(r)] = \kappa_e[n(r)] + \frac{1}{2} \iint \frac{n(r)n(r')}{|r-r'|} drdr' + \epsilon_{xc}[n(r)] + \int \nu_{en}(r)n(r)dr$$

- we minimize the above expression with respect to  $n(r)$  to obtain ground state energy and subject it to the constraint that the total number of electrons is constant i.e  $\int \delta n(r) dr = 0$  and as well as multiplying with a Lagrange multiplier  $\epsilon_i$

- the final Kohn sham equation is

$$\left\{ \frac{-\nabla^2}{2} + \nu_{\text{eff}}[n(r)] \right\} \phi_i(\mathbf{r}) = \epsilon_i \phi_i(\mathbf{r})$$

- the effective potential  $\nu_{\text{eff}}[n(r)]$  is given by

$$\nu_{\text{eff}}[n(r)] = \nu_{\text{en}}(r) + \int \frac{n(r')}{|r-r'|} dr' + \frac{\delta \epsilon_{\text{xc}}[n(r)]}{\delta n(r)}$$

- 1st term represents external potential due to ions, 2nd term is Hartree potential and 3rd term represents the exchange-correlation potential, note that the 3rd is not known exactly so its usually approximated:

$$\nu_{\text{xc}}[n(r)] = \frac{\delta \epsilon[n(r)]}{\delta n(r)}, \nu_{\text{xc}}$$

represents the electron-electron interaction not accounted by the Hartree term

### 2.3.4 Self-Consistent Field/Procedure for dft

self-consistent procedure for dft

1. Guess the initial electron density  $n$
2. calculate the Hartree and exchange correlational function from the pseudo-potential for each type of element present
3. Find the effective potential
4. use the above steps to solve the Hamiltonian and find the eigen values and eigen vectors to it
5. find the corresponding wave function and their electron density
6. Compare this with the initial value for a set error bar
7. If it lies outside this then use this new electron density as your new initial electron and repeat from step 1 onwards
8. this is done until the initial and final electron density are within our error bar, once we reach this stage we have successfully got our Ground state energy of the system

□

<sup>1</sup>self consistent image reference source <http://shialchemy.blogspot.com/2012/09/scf-loop-in-quantum-espresso.html>

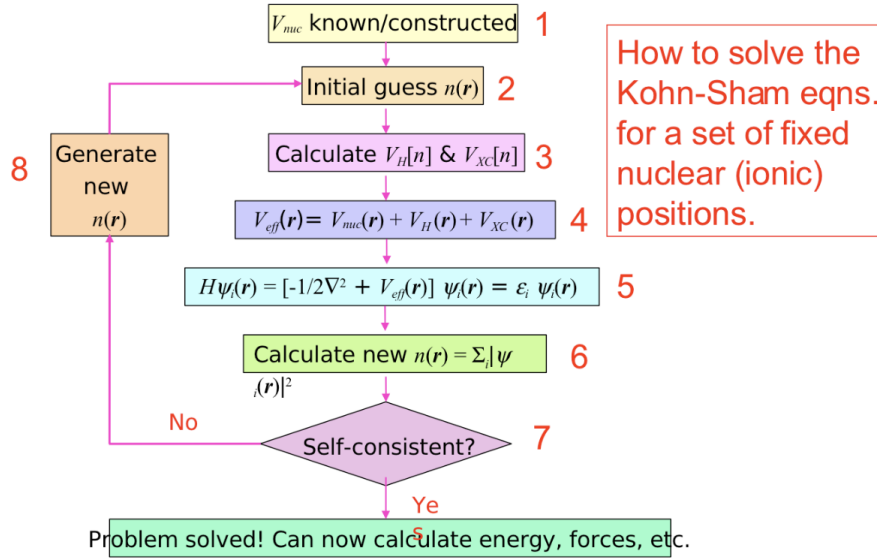


Figure 2.2: scf procedure for dft

### 2.3.5 Pseudo-potentials: a need and its types

- 1. Pseudo-potential:** The underlying potential experienced by electrons in solid has complex structure. An alternative potential is used to replicate the core electrons potential and produce an artificial potential that roughly approximates the valence electron potential and produces a smoother potential. It is used to simplify dft calculations and approximate the unknown  $E_{xc}$  of the material and it is used to replace the inter nuclear-electron term in our original Hamiltonian and Kohn Sham total energy with the pseudo-potential term is written as

$$E_{KS}[\rho] = T_s[\rho] + \int \rho(r)V_{ext}(r)dr + \sum_I \int \rho_I(r)V_{ps,I}dr + E_{XC}[\rho]$$

$T_s$  is the kinetic energy of a non-interacting electron,  $\rho_I(r)$  is the partial electron density associated with the pseudo-potential for nucleus I,  $V_{ps,I}$  is the effective potential associated with the pseudo-potential for nucleus I [5]

2. it can categorized into 3 main types of pseudo-potential

- **norm conserving pseudo-potentials** in this method a pseudo-wave-function is constructed that matches or is highly identical to the all-electron(real wave-function ) wave-function after a radius  $r_c$ , they share the same eigenvalues, the same probability for all electron orbital and pseudo orbital, the norm between the all-electron orbital and pseudo orbital is approximately 1 .we use it when we desire high accuracy, for optical properties of the material, bandstructure and electronic properties, when we wish to conserve the norm, defects behaviour and surface of a material
- **ultrasoft pseudopotentials** it is a method in which the norm condition is relaxed and fewer numbers of plane waves are used and produces a smoother pseudo-potential compared to norm-conserving pseudopotential. we can use it to study broader cases of elements without recalibration while giving a good balance of accuracy, convergence and efficiency

- **PAW(projector augmented wave)**: In this method, we approximate the true electron wave function with a combination of localized atomic wave-like function and pseudo wave function. we use the atomic wavelike function inside the core electron region and accurately describe the true wave function while we use the pseudo wave function to describe the true wave function outside the core wave region which is smoother and closely approximates the true electron wave function of the material being considered [6]

### 2.3.6 exchange-correlational approximation

there are two main approximations for exchange correlational namely **local density approximation:(LDA)** and **generalized gradient approximation:(GGA)**

1. LDA:it's an approximation for the exchange-correlation functional  $\epsilon_{xc}[n(r)]$  in a uniform electron gas(free electron gas).*it states that if the  $n(r)$  is slowly varying then the exchange-correlation of this density is equal to the exchange-correlation in a uniform free electron gas*

$$\epsilon_x^{\text{LDA}}[\mathbf{n}(\mathbf{r})] = \int \epsilon_x(\mathbf{r})\mathbf{n}(\mathbf{r})d\mathbf{r} \quad \text{where exchange energy } \epsilon_x(r) = C_2 n^{\frac{1}{3}}(r)$$

exchange potential is given by

$\nu_x[n(r)] = \frac{4}{3}C_2 n^{\frac{1}{3}}(r), C_2 n^{\frac{1}{3}}$  is effective electron-electron interaction due to exchange potential for a many body system we also need to include the correlation term as well, so the

$$\epsilon_{xc}^{\text{LDA}}[n(r)] = \int [\epsilon_x(r) + \epsilon_c(r)]n(r)$$

2. *shortcomings of LDA*: it does not work if  $n(r)$  varies rapidly and if  $n(r)$  shows spin-dependent behaviour
3. **GGA** the most significant extension added to LDA is the generalized gradient approximation **GGA** by **Pedrew, Burke and Erzerhof** deals by taking energy as a function of the electron density, gradient  $n(r)$ , spin term
4. the exchange term is written as,  $\epsilon_x^{\text{GGA}}[n(r)] = \int \epsilon_x n(r) F_x(s) dr$  and the correlation term is written  $\epsilon_c^{\text{GGA}}[n(r)] = \int [\epsilon_c n_{uni}(r) + H[n, \zeta]]n(r)$ , where  $\zeta$  is the relative spin polarization

### 2.3.7 limitations of LDA and GGA

they always underestimate the band gap of the material, this since there's a discontinuity in exchange potential which LDA+GGA does not account for due to them being smooth functions and local function of  $n(r)$  which give  $\Delta_{xc} = 0$  at the discontinuity of exchange potential

## 2.4 vdw correctionals

these vdw corrections are added to the  $E_{xc}$  to account for the long-range van der Waals interaction of the materials such as graphene. The main focus of vdw correctional functionals will be vdw-df2 and vdw-df-c6 which will be compared to pbe

### 2.4.1 vdw-df2

in vdw-df2 we modify the exchange-correlational such that it is a function of the usual stuff in GGA approximation along with some non-local functionals to account for the vdw forces, mathematically it is written as

$$E_{xc} = \int n(\mathbf{r}) \varepsilon_{xc}^{vdw-df2}(n(\mathbf{r}), \nabla n(\mathbf{r}))$$

here  $\varepsilon_{xc}^{vdw-df2}$  represents exchange-correlation energy per electron as a functional of  $n(\mathbf{r})$  and  $\nabla n(\mathbf{r})$ .

$$\varepsilon_{xc}^{vdw-df2} = \varepsilon_{xc}^{LDA} + \varepsilon_{xc}^{nl}$$

where  $\varepsilon_{xc}^{nl}$  represents the non-local correlational energy which accounts for the vdw interactions and is a function of  $n(\mathbf{r})$  and  $\nabla n(\mathbf{r})$

$$\text{mathematically } \varepsilon_{xc}^{nl} = \int d^3r \int d^3r' n(\mathbf{r}) \phi(r, r') n(\mathbf{r}')$$

where  $\phi$  is called the internal functional and is semilocal which takes care of the  $\varepsilon_{xc}$  of a gradient-corrected LDA at point  $\mathbf{r}$  [7]

### 2.4.2 vdw-df-c6 or c6

vdw-df-c6 or c6 takes care of the London dispersion forces. we do this by modifying our  $E_{xc}$  term

$$E_{xc}^{c6} = E_{xc}^{dft} + E_{disp}$$

where  $E_{xc}^{dft}$  is the standard exchange-correlation energy without any corrections and  $E_{disp}$  is the energy of the London force/dispersion force between two atoms or molecules at  $i$ th and  $j$ th position [8]

$$E_{disp} = \sum_{i < j} \frac{C_{6i,j}}{R_{i,j}^6}$$

where  $C_6$  is the coefficient of the dispersion relation between any two atoms (molecules) at the  $i$ th and  $j$ th positions.

$$C_6 \text{ is calculated in QE by } C_6 = \frac{-\partial^2 E_{xc}}{2\partial n^2}$$

## 2.5 limitations of dft

it can not be used in strongly correlated systems like liquids, ferromagnetic systems etc. strongly correlated meaning system where the coulombic or potential term dominates over the kinetic energy term. variational principle can't be used to refine the results because the  $\nu_{xc}$  is very sensitive to the initial input. It gives incorrect results for long non-covalent interactions example hydrogen bonding,  $\pi - \pi$  stacking. Struggles with dynamic systems where nuclear-electron coupling can't be ignored, non-static electron density, nuclear and electron speeds are relative to one another. requires in-depth knowledge of the material to select the correct XC functional which may not be suitable for other materials and other parameters which isn't always possible in simpler words your chosen parameters have to be finely tuned for different types of material.

# Chapter 3

## Results

### 3.1 Mono-Layer Graphene (MLG)

from the figure below we can see that MLG is a honeycomb structure (simple hexagonal) [9]. also, we keep the inter-unit distance  $c \sim 10$  or  $15 \text{ \AA}$  to ensure the interaction between any two unit cells is very weak and can be approximated to a non-interacting system.

The initially chosen coordinates for Graphene are  $(1/3, 2/3, 1/2)$  and  $(2/3, 1/3, 1/2)$

.The experimental value of lattice constant  $a$  is  $\sim 2.46 \text{ \AA}$ , band gap of  $0 \text{ eV}$ .

#### 3.1.1 structure for graphene

pseudopotential	type of approximation	lattice constant in $\text{\AA}$
C.pbe-n-kjpaw_psl.1.0.0.UPF	GGA+PAW	2.46

Table 3.1: pseudopotential, approximation and lattice constant

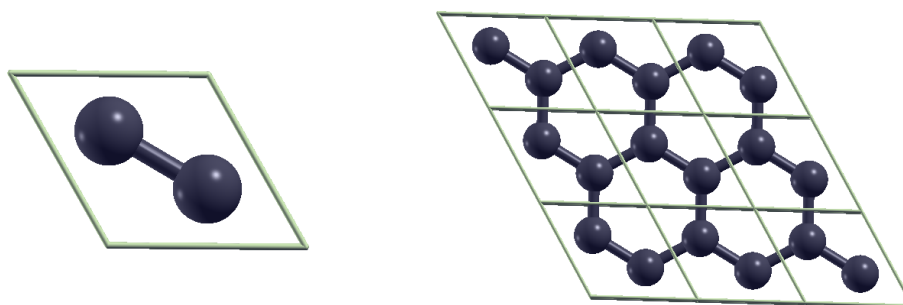


Figure 3.1: structure for unit cell for MLG and its extended version 3x3x1

we can see that the lattice obtained and experimental are in good agreement with one another.

## 3.2 Optimization

**K-points optimization:** it is the points in the reciprocal lattice with a constant equal spacing of  $2\pi/a$ . it's a grid  $k*k*k$  that is numerically integrated in the 1st Brillouin zone and used to determine the energy, electronic properties, and other properties of the material. It is optimized to reduce the number of k points required to save computational time and storage along with high-accuracy results. the optimized k points are carried by plotting k points vs scf energy and finding the point at which the energy saturates at points with very low fluctuations, this point is the optimized k point grid. note that k points don't strictly decrease monotonically but oscillate near the saturation point [5]

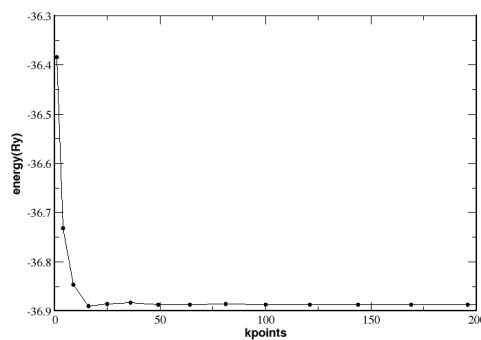


Figure 3.2: K-point graph using PAW pseudo-potential

**Ecut:** it's the maximum allowed kinetic energy of the plane waves being used within a radius  $r_c$ . it helps to determine the number of plane waves used for DFT calculations within the given k grid space, high ecut value gives a highly accurate result but it is computationally slow and takes a huge amount of storage which is the reason we optimize ecut value. it's optimized similarly to k-point optimization

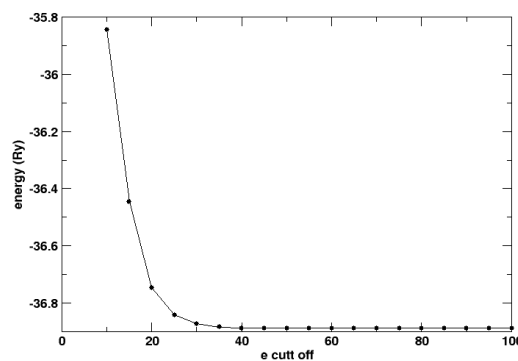


Figure 3.3: ecut graph for PAW

**smearing:** it's the artificial smoothing of electron density near the fermi level for metals is known as *smearing*. smearing is done to prevent the fluctuations of electron density for metals and metal-like materials during scf calculations. These fluctuations are caused due to the electrons near the fermi which can cross to the conduction band in one calculation and remain at the valence band in the other which causes the scf calculations to give incorrect results, it's done by creating smooth artificial function of energy running from 0 to 1 to help stabilize the fluctuations of electron density. smearing is optimized by carrying out scf calculations with different smearing functions with different values of the smearing function (degauss) and plotted against the energy, the one which fluctuates the least is the optimized smearing function

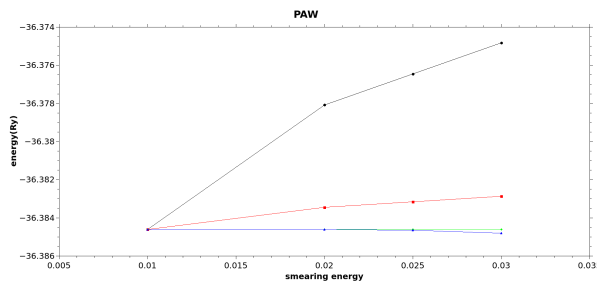


Figure 3.4: smearing here for PAW

all these steps along with relaxation(optimization of the unit cell) are to create an optimized scf file from which our band structure and DOS are obtained from which the electronic properties of the materials and other properties are inferred on and interpreted

### 3.3 excitation spectra

**Bandstructure:** the range of energy in a continuum in which electrons may occupy is called band structure otherwise it's also called the energy dispersion relation, this is a function of the  $\mathbf{K}$ . band structure is useful for telling whether the material is a metal, semiconductor, or insulator. it's calculated by first running scf calculations and finding the energy of each electron, then performing an NSCF calculation to extract the eigen values and eigen vectors of those energies and convert them into a .gnu file and extract the data from there, subtract the Fermi energy we obtain with the bandstructure so that the zero aligns itself with the Fermi level. we use an external plotting application (Xmgrace/QTiplot) to plot and interpret the data obtained

The experimental band gap for un-doped graphene is 0 eV and the one obtained is 0 eV. Also, note that the experimental band gap obtained and the one we obtained from our DFT calculation perfectly match each other. Note that the valence bands are filled and just touch the conduction bands at the Fermi level. This point is reported in the literature review as the Dirac point

**Density of states(DOS):** it's the energy occupied at a given electronic for a given dimension. DOS is useful for telling how the number of electronic states is distributed within a given dimension(0-3) at a given energy. it's carried by first running a scf calculation and then we use this scf energies to integrate

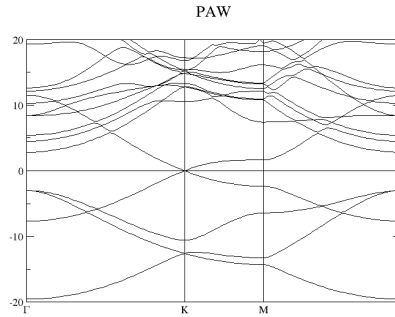


Figure 3.5: bandstructure of PAW

them using the *tetrahedron method*. In this method, the grid is subdivided into many tetrahedrons and then numerically integrated to give the DOS of the system, we then use the DOS.x commands to convert this output into a spreadsheet which is then plotted against the energy. We also subtract the Fermi level from here to make the 0 align with the Fermi level. This plot is then accordingly interpreted. We have chosen 4 High symmetry points  $\Gamma(k=0)$ ,  $K(k=0.6667)$ ,  $M(k=1.000)$ ,  $\Gamma(k=1.577)$

The DOS at Fermi level is 0 at the Fermi level.

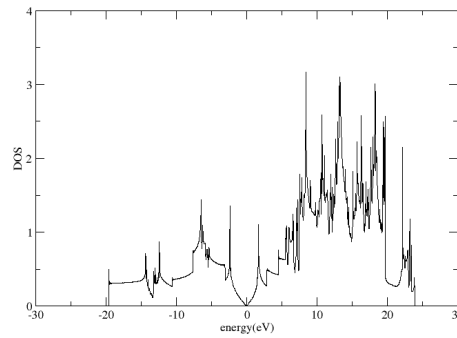


Figure 3.6: DOS of PAW

The DOS, band gap is 0 which is in line with the previous studies done.

### 3.4 Bi-layer Graphene(BLG)

For *BLG* we have two layers of Graphene sheets separated by a distance  $d$  in a single unit cell which has the same C-C bond length of  $1.42 \text{ \AA}$  because we have taken the same material and have increased the number of layers. [10].

### 3.4.1 AA Stacking

#### Structural Optimization and Relaxation

In AA stacking the graphene layers are perfectly aligned on top of each other. We have performed structural relaxation optimization and found we optimized the K point grid, ecut and smearing. [9]



Figure 3.7: AA stacking structure: unit cell and 3x3x1

parameter	K point	Ecut	Smearing
optimized value	72	50	MP

Table 3.2: optimized value for AA structure

Experimentally AA and AB have an inter-layer distance of 3.55 and 3.55 Å respectively from the

vdw functional	pbe	df2	c6
lattice constant in Å	2.46	2.49	2.46
fermi energy in eV	3.32	3.07	3.20
C-C bond length in Å	1.42	1.44	1.42
inter-layer distance in Å	4.38	3.61	3.43
relative error in inter-layer distance in %	23	1.7	3.4

Table 3.3: Data for different vdw functionals for AA

given data we can see that overall C6 is the best one over here for describing AA BLG. This was used to calculate the band gap and DOS for pure AA and the obtained lattice parameters within 1.2 % of the experimental value [3]

#### Band structure and DOS for AA stacking

we can see that the band structure of AA has a symmetric split at the K symmetry point with a band gap of 0.1 eV This is explained due to the electronic inter-layer coupling. All 3 vdw show similar results for the band gap

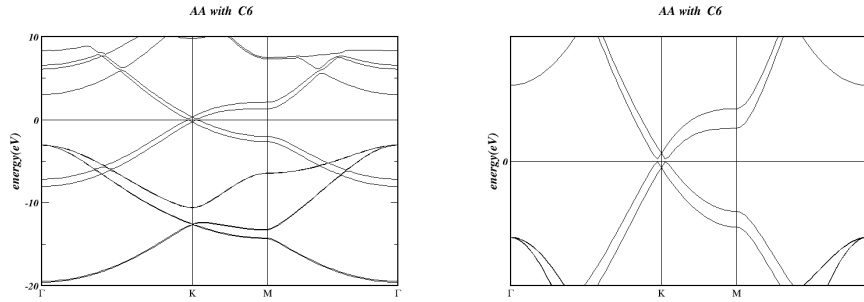


Figure 3.8: Band-structure for AA stacking with c6 vdw correctional and its zoomed version.-20 eV to 10 eV for the 1st image, right one is -5 to 5 eV range

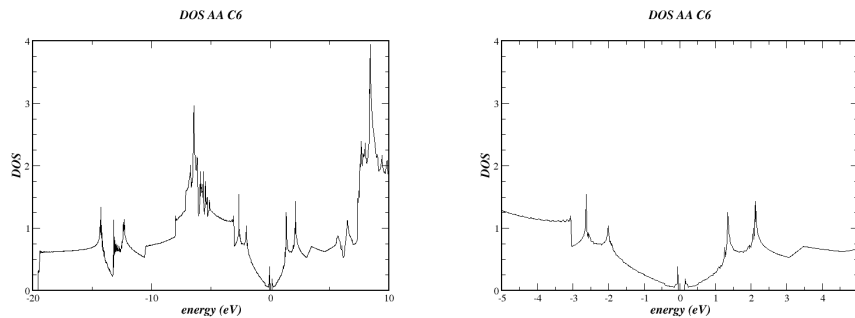


Figure 3.9: The DOS of the above figures with the same energy range

vdw used	pbe	df2	c6
band gap in eV	0.11	0.03	0.11

Table 3.4: band gap with different vdw functionals for AA stacking

### 3.4.2 AB stacking

In AB stacking the 1st and 3rd layers are perfectly aligned while the 2nd layer and 4th layers are perfectly aligned. B layer the hexagonal structure is slightly shifted to the centre of the vacant space in the A layer. This type of stacking is also known as Bernal stacking otherwise commonly called AB Stacking. This stacking is the most preferred form of stacking by graphene in nature [11]

parameter	K point	Ecut	Smearing
optimized value	72	50	MP

vdw functional	pbe	df2	c6
lattice constant	2.46	2.49	2.46
Fermi energy in eV	3.31	3.06	3.18
C-C bond length in Å	1.42	1.44	1.42
inter-layer distance in Å	3.70	3.56	3.42
relative error in inter-layer distance in %	10.38	6.2	1.95

Table 3.5: lattice constant, energy obtained for different vdw functionals for AB

from the given data we can see that df2 gives the result

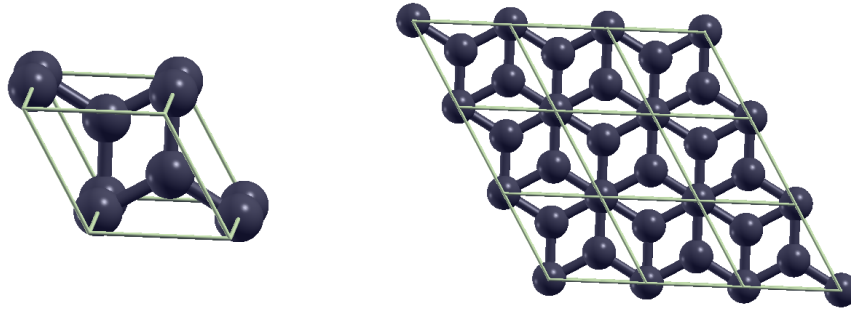
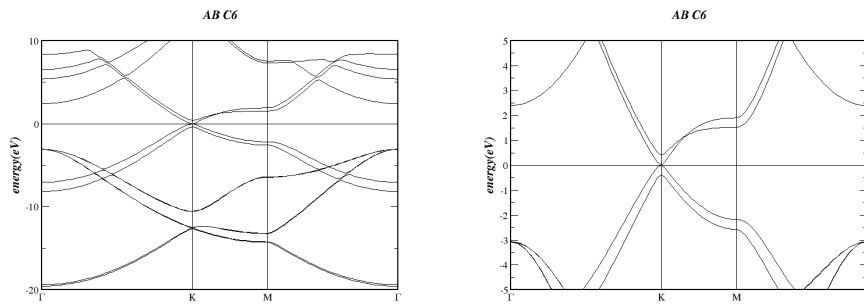


Figure 3.10: AB stacking: unit cell and 3x3x1

### Band gap and DOS for AB stacking

Figure 3.11: Band structure for AB stacking with  $c_6$  vdW. energy range for the left one is -20 to 10 eV, right one is -5 to 5 eV

This band nature can be explained since the lowest conduction and highest valence band meet exactly at the fermi level.

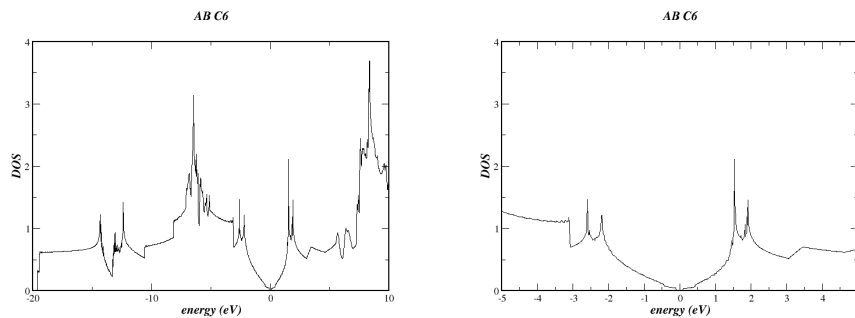


Figure 3.12: DOS of the above figure with the same energy range

vdw used	pbe	df2	c6
band gap in eV	0	0	0

Table 3.6: band gap with different vdw functionals for AB stacking

### 3.4.3 Comparison between AA and AB stacking

band gap for AA and AB stacking

stacking	pbe	df2	c6
AA	0.11 eV	0.03 eV	0.11 eV
AB	0 eV	0 eV	0 eV

Table 3.7: band gap for different vdw functionals with AA and AB stacking for bi-layer graphene

AA has a band gap due to increased coulombic repulsion between the pz electrons and slightly less overlap between them for vdw forces. This leads AA to have less stability as compared to AB, this can be observed from scf calculation that AA has an energy of -47.34 and AB has an energy of -47.89

inter layer distance

stacking	pbe	df2	c6
AA	4.3786	3.6141	3.4313
AB	3.6976	3.5578	3.4152

Table 3.8: inter-layer distance in Å for BLG

**The Comparison of the inter-layer distance for AA and AB** if we compare the experimental and our obtained values for inter-layer distance, We can see that AA has more inter-layer distance than AB. This is due to AA having a stronger repulsion from the pz electrons bands than AB

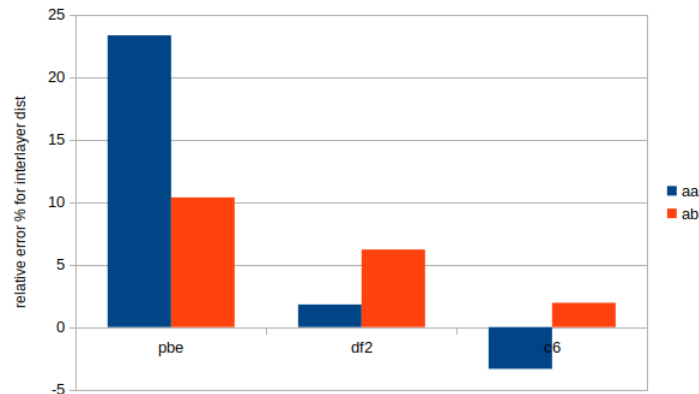


Figure 3.13: relative error for inter-layer distance for AA and AB stacking for different vdw functionals; AA is blue while AB is orange. Experimental value for AA =3.55 Å and for AB=3.35 Å

from the above results, we can see that AB stacking for BLG gives identical results to graphite. At the same time, AA is almost identical to AB aside from the symmetry breaking at the high symmetry

point at K. Also it can be seen that vdw plays a significant role in determining the inter-layer distance and band gap. We can see that df2 gives the most accurate result for AA and c6 gives the most accurate result for Ab stacking. Even though AA Stacking has a band gap a very small one is almost identical to AB stacking. The small splitting that we have observed in both AA and AB is due to the inter-layer coupling present in BLG

## 3.5 Doping

### 3.5.1 Comparison between un-doped and doped MLG

a super-lattice of  $2^*a$  for MLG, BLG was constructed with the help of burai and then later optimized using QE, this was then doped with N with the ratio of 1 N atom:7 C atoms for each layer, this doped super-lattice was optimized and then studied for its electronic properties. N was chosen to be a dopant due to the similar properties to C, high abundance, high carrier mobility, etc [12] [4]. The decrease in lattice constant can be explained due N's higher electro-negativity.

pseudo-potential	type of approximation	lattice constant in Å
N.pbe-n-rrkjus_psl.1.0.0.UPF	GGA+US	4.89
C.pbe-n-rrkjus_psl.0.1.UPF	GGA+US	4.93

Table 3.9: pseudo-potential, approximation, and lattice constant

#### structure of doped and undoped graphene

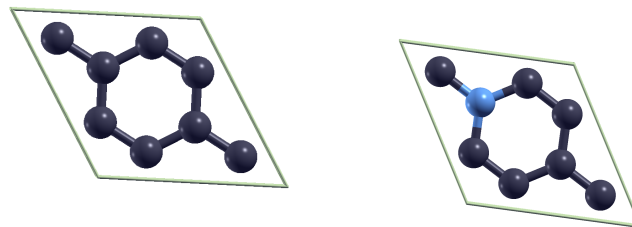


Figure 3.14: structure of undoped and doped monolayer graphene

#### Band-structure and DOS OF Undoped AND Doped MLG

. From the given figure we can see that the band gap has completely disappeared for Doped BLG and now become metallic

bond type	bond length in Å
N-C	1.414
C-C( near N atom)	1.413
C-C(away from N atom)	1.408

Table 3.10: obtained bond length for N doped MLG

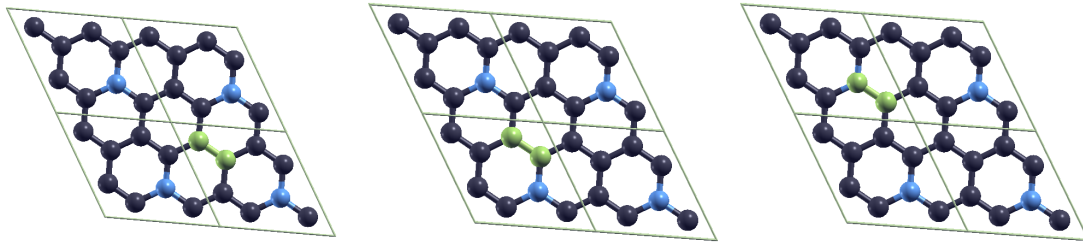


Figure 3.15: The different bond length diagram C-C ( N far), C-C(N near), N-C. atoms in green represent the selected atoms

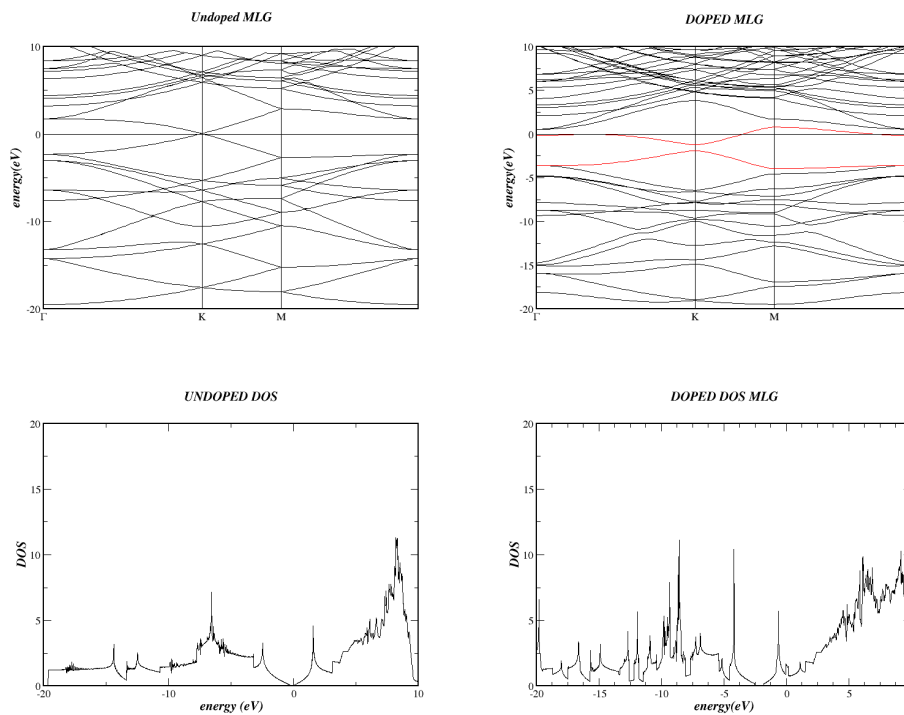


Figure 3.16: band structure and DOS of undoped and doped MLG.the red line is the lowest conduction and highest valence band respectively

type	undoped	1N doped
lattice constant	4.93	4.89
fermi energy in eV	-1.7219	-0.6035
DOS at fermi level	0	3.65

Table 3.11: properties of undoped and doped MLG

. We have noticed that the lattice parameter has gotten smaller, this is expected behaviour due to the higher electro-negativity of N than that of C. The change in the Fermi energy can be attributed to the change in carrier concentration in MLG which has an equal number of electrons and holes but when doped with N the concentration of electrons has increased and the number of holes has remained the same, shifting the fermi energy closer to the conduction band now. The DOS which has changed from a

zero for undoped to a non-zero value for the DOS [13] [14]

### 3.6 N-DOPED BI-LAYER GRAPHENE: N DOPED BLG

We will use the same pseudo-potential as before and keep the ratio of 1:7 per layer for our N-doped BLG calculation. We used a 200 k grid with an ecut of 80 Ry with MP smearing.

vdw used	pbe	df2	c6
lattice constant Å	4.89	4.94	4.89
N-C bond length in Å	1.41	1.43	1.41
C-C bond length in Å	1.41	1.42	1.41

Table 3.12: N-doped AA BLG data

vdw used	pbe	df2	c6
lattice constant Å	4.89	4.94	4.89
N-C bond length in Å	1.42	1.43	1.42
C-C bond length in Å	1.41	1.42	1.41

Table 3.13: N-doped AB BLG data

#### Structure of AA and AB N-doped BLG

structure of AA and AB stacked N doped BLG

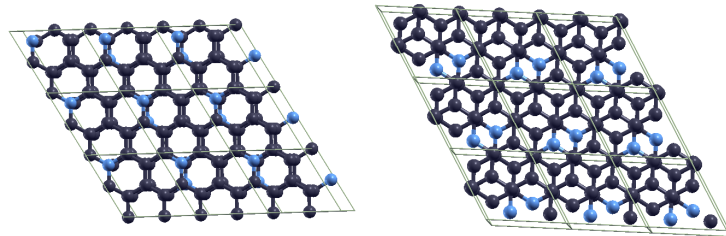


Figure 3.17: . we have used 3x3x1 repetition of the unit is used here

#### Inter-layer distance

##### NOTE

1. C-C (Near N) refers to the C-C bonds that have at least one N attached adjacent to one of the C
2. C-C (Far N) refers to C-C bonds that have no N attached adjacent to these C atoms under consideration
3. The order is as follows for the pictures: C-C (N far), C-C(N near), N-N, N-C

With the inclusions with df2 and c6 as vdw correction functionals, the inter-layer has reduced drastically and AA is now much lower than AB and for C6 we get the minimum amount of inter-layer distance

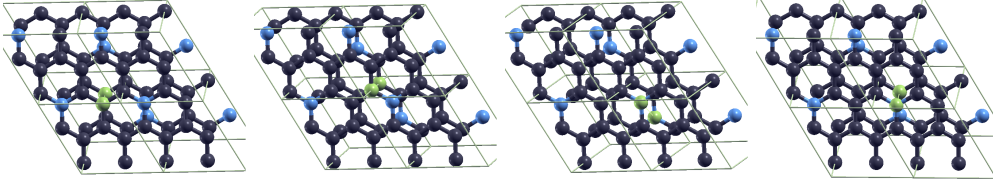


Figure 3.18: different interlayer distance for different types of bonds for AA.

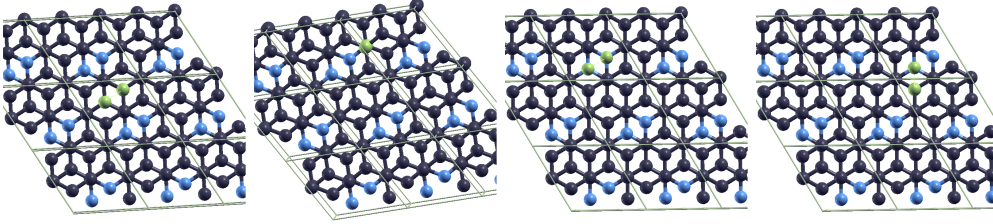


Figure 3.19: different interlayer distance for different types of bonds for AB.

Stacking	AA	AB
C-C(Near N) in Å	6.0342	4.2795
N-C in Å	6.0232	4.5058
C-C(Far N) in Å	6.0317	4.506
N-N in Å	6.6615	4.5044

Table 3.14: inter-layer distance for N doped BLG with pbe

Stacking	AA	AB
C-C(N near) in Å	3.418	3.8003
N-C in Å	3.409	3.794
C-C(N far) in Å	3.4145	3.8025
N-N in Å	3.6886	3.7998

Table 3.15: inter-layer distance for N doped BLG with DF2

Stacking	AA	AB
C-C(N near) in Å	3.1225	3.2667
N-C in Å	3.1134	3.5561
C-C(N far) in Å	3.1163	3.5629
N-N in Å	3.411	3.5521

Table 3.16: inter-layer distance for N doped BLG with C6 for vdw interaction.

### Band structure of AA AND AB N-doped BLG

Without vdw corrections:pbe

Stacking	AA	AB
Fermi energy(scF) in eV	2.0264	4.6271
DOS at Fermi level	8.328	7.969

Table 3.17: DOS and Fermi energy obtained for AA and AB stacking for pbe

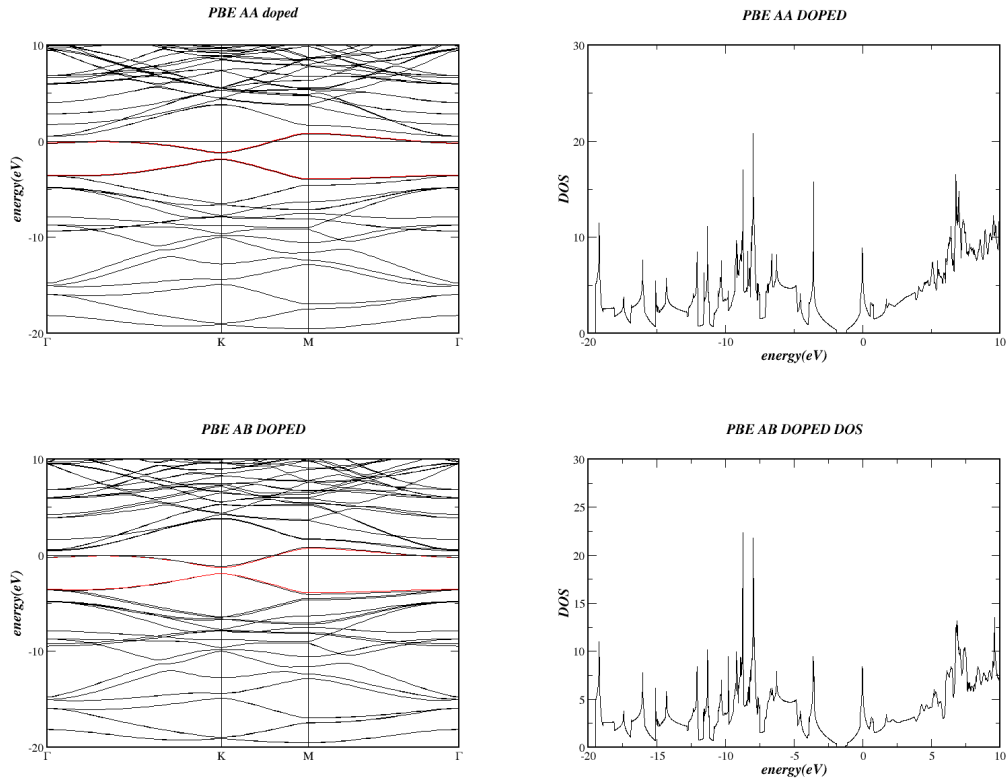


Figure 3.20: AA on the left-hand side and AB on the right-hand side

The same metallic nature of the band gap has been observed as in the case of N-doped MLG. The DOS at the Fermi level has increased by 49 and 46 % from the N-doped MLG this implies that N-doped BIG is highly more metallic than N-doped MLG. Also now the Fermi energy has significantly increased albeit there is a large discrepancy between AA and AB

with vdw corrections: Df2 and C6

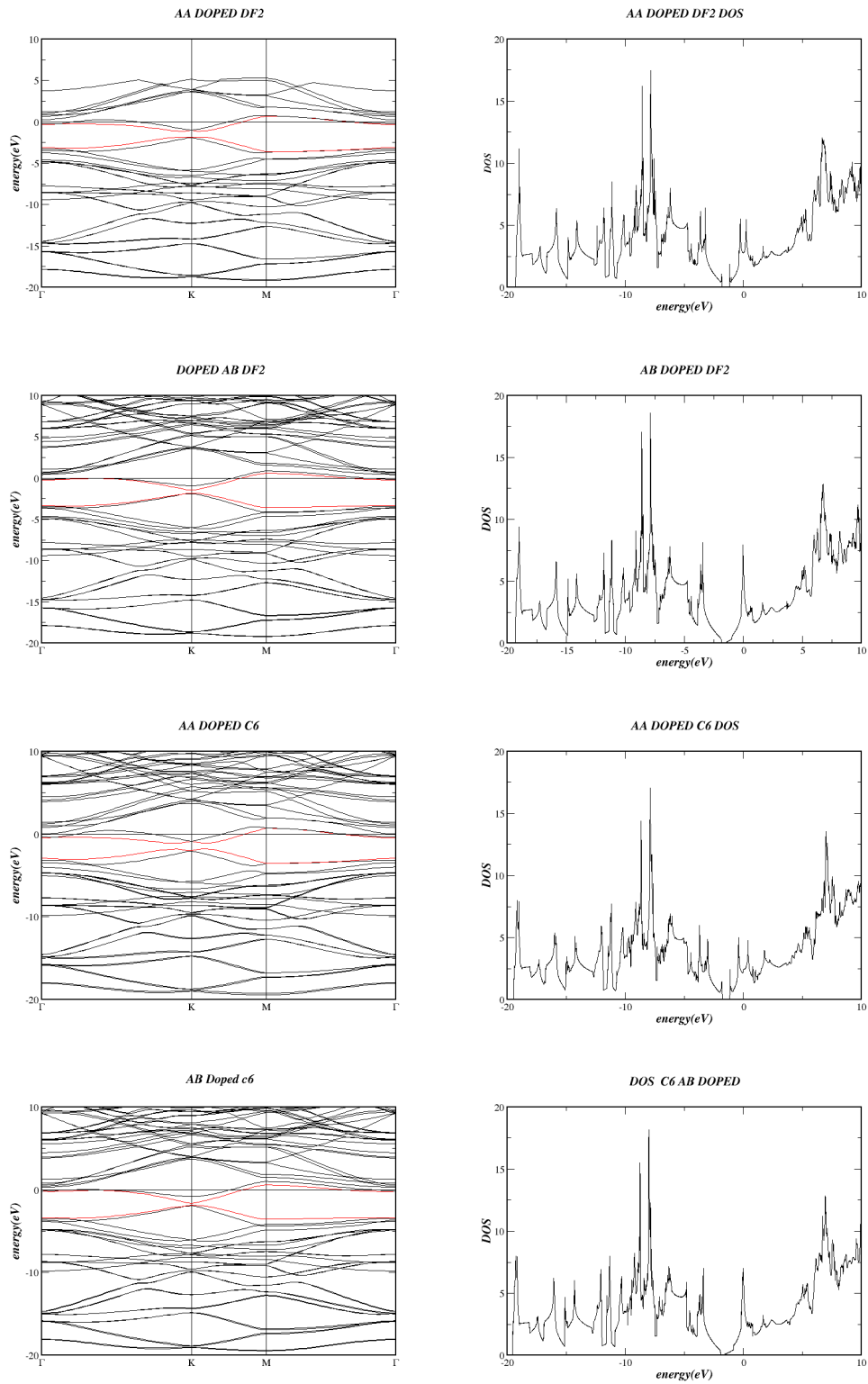


Figure 3.21: AA and AB stacking with df2 and c6 vdw correction

Stacking	AA	AB
Fermi energy(scF) in eV	4.1901	4.2468
DOS at Fermi level	2.776	6.866

Table 3.18: Fermi energy and DOS obtained for AA and AB stacking with df2

Stacking	AA	AB
Fermi energy(scF) in eV	4.369	4.4723
DOS at Fermi level	2.457	6.472

Table 3.19: Fermi energy and DOS obtained for AA and AB stacking with c6

On adding vdw correction df2 and c6 we see that the DOS for AA and AB has decreased sharply, the discrepancy between AA and AB has increased and the Fermi level has become comparable between AA and AB. AA has a lower DOS to N-doped MLG and vice versa for AB. we notice a downward trend from df2 to c6 in the Fermi energy for AA and AB and the opposite happens for DOS.

### 3.7 Summary

The electronic properties of Graphene were studied using Density Functional theory. Undoped Monolayer Graphene and undoped AB stacked Graphene showed zero Bandgap at high symmetry K point as well their DOS was found to be zero at the fermi level. The electronic repulsion by the pz electrons created a small band gap near the high symmetry K point which increased the inter-layer distance and created a small band gap for bi layer. Various Van der Waals functionals were used to increase the accuracy of the inter-layer distance and Band gap and to check the role of Van der Waals interaction in the inter-layer distance and band gap in bi layer graphene. We doped Graphene 2x2 super lattice with Nitrogen to 1:7 ratio per layer. This made it completely metallic and has a non-zero value of Density of states at the fermi level, AB Stacking increased the density of states at the fermi level compared to the doped mono-layer while a decrease in the density of states for AA stacking was observed. It also shifted the fermi level towards the conduction band.

# Bibliography

- [1] K. Burke J.P.Perdew and M. Ernzerhof. "generalized gradient approximation made simple. *Physical Review Letters*, 1996.
- [2] Andre Geim and Konstantin Novoselov. Electric field effect in atomically thin carbon films. *Science*, 2004.
- [3] M. Boujnah et al. Electronic and electrical conductivity of ab and aa-stacked bilayer graphene with tunable layer separation. *Research Gate*, 2016.
- [4] Adwaa Ahmed. First-principle analysis of the electronic and optical properties of boron and nitrogen-doped carbon mono-layer graphenes. *Research Gate*, 2014.
- [5] Riichiro Saito Nguyen Tuan Hung, Ahmad R. T. Nugraha. *Quantum ESPRESSO Course for Solid-State Physics*. Jenny Stanford Publishing, 2022.
- [6] Xavier Gonze and Fabio Finocchi. Pseudopotentials plane waves–projector augmented waves: A primer. *Physica Scripta*, 2004.
- [7] KARIM ELGAMMAL. Density functional theory calculations for graphene-based gas sensor technology. *KTH School of Engineering Sciences SE-164 40 KISTA, Stockholm, Sverig*, 2018.
- [8] K. Berland et al. Van der waals density functional with corrected c6 coefficients. *APS*, 2019.
- [9] A. H. Castro Neto, F. Guinea, N. M. R. Peres, K. S. Novoselov, and A. K. Geim. The electronic properties of graphene. *Rev. Mod. Phys.*, 81:109–162, Jan 2009.
- [10] Karolina Z. Milowska. Van der waals density functionals for graphene layers and graphite. *Research Gate*, 2011.
- [11] Eduardo V. Castro, K. S. Novoselov, S. V. Morozov, N. M. R. Peres, J. M. B. Lopes dos Santos, Johan Nilsson, F. Guinea, A. K. Geim, and A. H. Castro Neto. Biased bilayer graphene: Semiconductor with a gap tunable by the electric field effect. *Phys. Rev. Lett.*, 99:216802, Nov 2007.
- [12] Liuyan Zhao et al. Visualizing individual nitrogen dopants in monolayer graphene. *Department of Physics, Columbia University, New York NY 10027, USA*.
- [13] Nzar Rauf Abdullah. Controlling physical properties of bilayer graphene by stacking orientation caused by interaction between b and n dopant atoms. *ELSEVIER*, 2022.

- [14] A.L. Olatomiwa et al. Recent advances in density functional theory approach for optoelectronics properties of graphene. *Heliyon*, 2023.